



## Thermodynamic Analysis of Solar Absorption Cooling System

Jasim Abdulateef<sup>1,\*</sup>, Sameer Dawood Ali<sup>1</sup>, Mustafa Sabah Mahdi<sup>2</sup>

<sup>1</sup> Mechanical Engineering Department, University of Diyala, 32001 Diyala, Iraq

<sup>2</sup> Chemical Engineering Department, University of Diyala, 32001 Diyala, Iraq

### ARTICLE INFO

#### Article history:

Received 16 April 2019

Received in revised form 14 May 2019

Accepted 18 July 2018

Available online 28 August 2019

#### Keywords:

Refrigeration; absorption; solar collector;  
entropy generation; irreversible losses

### ABSTRACT

This study deals with thermodynamic analysis of solar assisted absorption refrigeration system. A computational routine based on entropy generation was written in MATLAB to investigate the irreversible losses of individual component and the total entropy generation ( $\dot{S}_{tot}$ ) of the system. The trend in coefficient of performance  $COP$  and  $\dot{S}_{tot}$  with the variation of generator, evaporator, condenser and absorber temperatures and heat exchanger effectivenesses have been presented. The results show that, both  $COP$  and  $\dot{S}_{tot}$  proportional with the generator and evaporator temperatures. The  $COP$  and irreversibility are inversely proportional to the condenser and absorber temperatures. Further, the solar collector is the largest fraction of total destruction losses of the system followed by the generator and absorber. The maximum destruction losses of solar collector reach up to 70% and within the range 6-14% in case of generator and absorber. Therefore, these components require more improvements as per the design aspects.

Copyright © 2019 PENERBIT AKADEMIA BARU - All rights reserved

## 1. Introduction

With the onset of energy crises and the pressure from environment protection, solar energy technology can be considered the best option for daily activates nowadays [1,2]. In the domain of production cold or fresh air, the absorption refrigeration system (ARS) solutions are considered practically suited for solar applications [3-6]. Several optimization investigations using energy analysis are conducted. The energy analysis based on first law of thermodynamics deals with energy conversion in the absorption cycle. This cannot identify where the large destructions rate (entropy generation) take place.

The concept of second law of thermodynamics based on entropy generation is the only method to provide information of irreversibility losses in the various components of the system. Thus, the efficiency of the ARS can be improved by minimizing the total entropy generation [7-9]. Most research studies concern on solar assisted absorption refrigeration systems SAARSs with single stage type.

\* Corresponding author.

E-mail address: [jmabdulateef@gmail.com](mailto:jmabdulateef@gmail.com) (Jasim Abdulateef)

Chen and Schouten [10] performed an optimization study on ARS. They optimized the expression of *COP* for the irreversible ARS based on number of parameters for the system. Sözen [11] conducted an exergy analysis on ARS. The exergy losses in individual component is investigated based on performance parameters such as *COP*, exergetic coefficient of performance *ECOP* and circulation ratio. Chua *et al.*, [12] studied the energy analysis of NH<sub>3</sub>-H<sub>2</sub>O absorption system based on entropy generation and thermal conductance of heat exchangers. They found that the largest destruction rate in the rectifier.

Hasan *et al.*, [13] defined the second law efficiency of a reversible cycle and found the optimum operating conditions. The performance of the cycle was examined for the solar heat source temperature between 330 K- 470 K. Misra *et al.*, [14] applied the exergy based thermoeconomic technique on ARS. They optimized the absorption system that used for air conditioning applications. Kaynakli and Yamankaradeniz [15] carried out a detailed thermodynamic analysis of LiBr-H<sub>2</sub>O cycle. They concluded that the irreversible losses of the system inversely proportional with generator temperature. Rivera *et al.*, [16] performed a thermodynamic analysis on heat transformer with LiBr-H<sub>2</sub>O as a working fluid. They reported that the maximum values of performance parameters (*COP*, external *COP* and *ECOP*) are determined when the solution concentration up to 50%.

Fellah *et al.*, [17] conducted a study on the performance of SAARS to optimize the operating and design conditions in order to obtain the highest refrigeration effect. Tubreoumya *et al.*, [18] [2017] used the second law principle to detect the irreversible rates on SAARS. They built a numerical simulation based on the exergy analysis for individual components at different environment conditions. Bhaumik *et al.*, [19] developed a numerical program for energy and exergy analysis of LiBr-H<sub>2</sub>O absorption system. They reported that the maximum entropy generation existed in the generator and absorber.

Lavinia *et al.*, [20] used the exergy analysis to evaluate the performance of a combined cycle: organic Rankine cycle *ORC* and absorption cooling system *ACS* driven by solar energy. The results found that the exergy efficiency can be increased by use of a solution heat exchanger on *ACS*. In order to enhance the performance of *ORC* system, a recovery heat exchanger at the condenser inlet is required to add due to its high irreversibility losses. Maurice *et al.*, [21] analyzed the exergy destruction of SAARS. The performance parameters (*COP*, *ECOP*) of the system were calculated under selected weather conditions. They observed that the largest exergy dissipation occurred in the solar collector and generator. Soheil *et al.*, [22] studied the exergy analysis of ARS with consideration of water-lithium bromide as a working fluid. The simulation results indicated that the largest rate of destruction occurred in the absorber and reaches up to 36 % of the total destruction losses of the system.

Some development studies deal with double-effect absorption refrigeration system using principle of entropy generation minimization. Adewusi and Zubair [23] determined the entropy generation distribution of the entire NH<sub>3</sub>-H<sub>2</sub>O absorption system. They concluded that the destruction rate of two-stage ARS is greater than 50% of single-stage ARS. Ezzine *et al.*, [24] investigated the thermodynamic analysis of double stage absorption chiller driven by solar source. They quantified the losses rate at each component of the system. Kaushik and Arora [25] developed a simulation model for parametric investigation of single effect and series flow double effect ARS. The results showed that the performance of double effect system is greater about 60-70% than single stage ARS. The largest destruction rate was found in the absorber for both systems.

In this study, a thermodynamic analysis is used to investigate the performance of SAARS. The entropy generation distribution and the performance parameters of the SAARS are determined at different operating conditions. For this purpose, a simulation model was developed using MATLAB.

## 2. System Description

Figure 1 shows the schematic diagram of SAARS which is the main components of the system are the solar collector (*sc*), generator (*gen*), evaporator (*evp*), condenser (*cond*), absorber (*abs*), refrigerant heat exchanger (*RHX*) and solution heat exchanger (*SHX*), pump (*p*), refrigerant expansion valve (*V1*) and solution expansion valve (*V2*).

The working pair used in the present system is LiBr-H<sub>2</sub>O. The heat collected by solar collector is used as a heat input to the generator ( $Q_{gen}$ ). The heat is rejected from condenser ( $Q_{cond}$ ) and absorber ( $Q_{abs}$ ) to the cooling water, Eq. (13)-(16). The heat rate ( $Q_{evp}$ ) is transferred from cooling space to the evaporator, Eq. (17) and (18). The liquid solution that coming from the absorber is then pumped to the generator through *SHX*, Eq. (1)-(3). When the heat applied by the collector is absorbed by the generator, the refrigerant in the solution is driven out and goes to the condenser, Eq. (7) and (8). The refrigerant passes through (*RHX*) and then expands through (*V1*) and proceeds to the evaporator. The performance of the cycle can be improved by increasing the temperature, Eq. (2) and decreasing the temperature, Eq. (4) using *SHX* where the solution coming from *SHX* passes to the absorber at low pressure through (*V2*), Eq. (5) and (6).

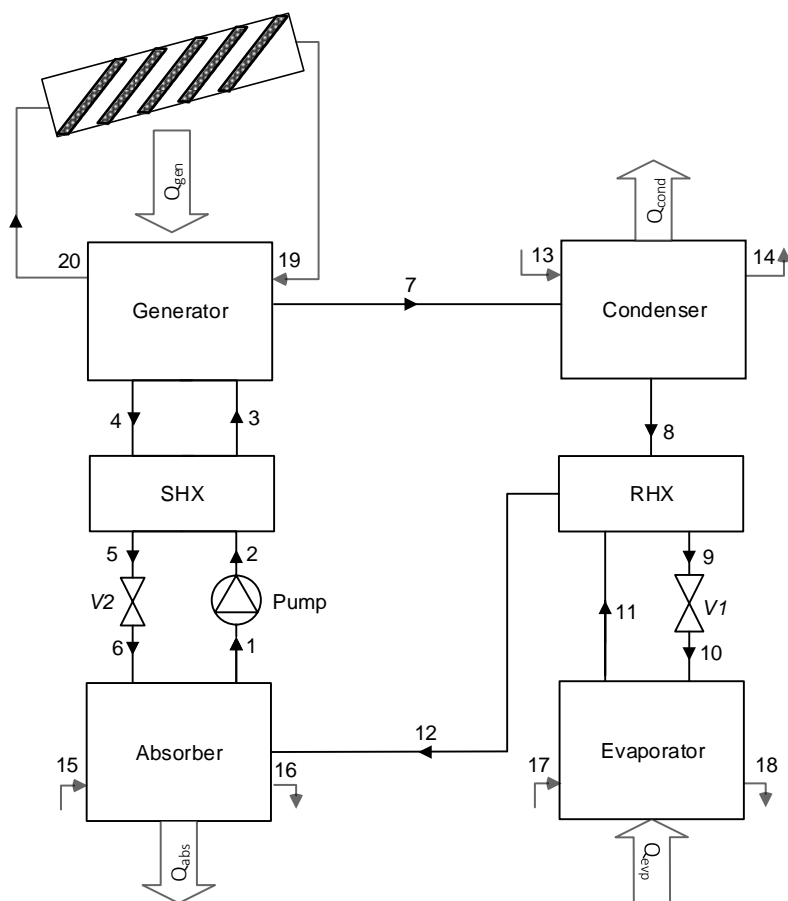


**Fig. 1.** The schematic illustration of the SAARS

## 3. Thermodynamic Analysis

The performance equations based upon the first and second law of thermodynamics can be applied for each component of the system. The equations of first law is written based on energy

balance. In the second law, the destruction losses in the system is considered due to the entropy generation [26]. The specified state points in the equations are related to the Figure 1.

#### Solar collector

$$\dot{Q}_{sc} = \dot{m}_{19}(h_{19} - h_{20}) \quad (1)$$

$$\dot{S}_{sc} = \dot{m}_{19}(s_{19} - s_{20}) - \frac{\dot{Q}_{rad}}{T_{sc}} \quad (2)$$

#### Generator

$$\dot{Q}_{gen} = \dot{m}_4 h_4 + \dot{m}_7 h_7 - \dot{m}_3 h_3 \quad (3)$$

$$\dot{S}_{gen} = \dot{m}_4 s_4 + \dot{m}_7 s_7 + \dot{m}_{20} s_{20} - \dot{m}_3 s_3 - \dot{m}_{19} s_{19} \quad (4)$$

#### Evaporator

$$\dot{Q}_{evp} = \dot{m}_{11}(h_{11} - h_{10}) \quad (5)$$

$$\dot{S}_{evp} = \dot{m}_{11} s_{11} + \dot{m}_{18} s_{18} - \dot{m}_{10} s_{10} - \dot{m}_{17} s_{17} \quad (6)$$

#### Condenser

$$\dot{Q}_{cond} = \dot{m}_7(h_7 - h_8) \quad (7)$$

$$\dot{S}_{cond} = \dot{m}_8 s_8 + \dot{m}_{14} s_{14} - \dot{m}_7 s_7 - \dot{m}_{13} s_{13} \quad (8)$$

#### Absorber

$$\dot{Q}_{abs} = \dot{m}_6 h_6 + \dot{m}_{12} h_{12} - \dot{m}_1 h_1 \quad (9)$$

$$\dot{S}_{abs} = \dot{m}_1 s_1 + \dot{m}_{16} s_{16} - \dot{m}_6 s_6 - \dot{m}_{12} s_{12} - \dot{m}_{15} s_{15} \quad (10)$$

#### Refrigerant heat exchanger (RHX)

$$\varepsilon_{RHX} = \frac{T_{11} - T_{12}}{T_{11} - T_8} \quad (11)$$

$$\dot{Q}_{RHX} = \dot{m}_8(h_8 - h_9) = \dot{m}_{12}(h_{12} - h_{11}) \quad (12)$$

$$\dot{S}_{RHX} = \dot{m}_9 s_9 + \dot{m}_{12} s_{12} - \dot{m}_8 s_8 - \dot{m}_{11} s_{11} \quad (13)$$

#### Solution heat exchanger (SHX)

$$\varepsilon_{SHX} = \frac{T_4 - T_5}{T_4 - T_2} \quad (14)$$

$$\dot{Q}_{SHX} = \dot{m}_4(h_4 - h_5) = \dot{m}_3(h_3 - h_2) \quad (15)$$

$$\dot{S}_{SHX} = \dot{m}_3s_3 + \dot{m}_5s_5 - \dot{m}_2s_2 - \dot{m}_4s_4 \quad (16)$$

Solution pump

$$\dot{W}_p = \dot{m}_2(h_2 - h_1) \quad (17)$$

$$\dot{S}_p = \dot{m}_2(s_2 - s_1) \quad (18)$$

Refrigerant expansion valve (V1)

$$\dot{m}_9h_9 = \dot{m}_{10}h_{10} \quad (19)$$

$$\dot{S}_{V1} = \dot{m}_{10}(s_{10} - s_9) \quad (20)$$

Solution expansion valve (V2)

$$\dot{m}_5h_5 = \dot{m}_6h_6 \quad (21)$$

$$\dot{S}_{V2} = \dot{m}_6(s_6 - s_5) \quad (22)$$

The total entropy generation rate of the SAARS is the sum of the entropy generation rate in each component, therefore:

$$\dot{S}_{tot} = \sum_{i=1}^N \dot{S}_i = \dot{S}_{sc} + \dot{S}_{gen} + \dot{S}_{evp} + \dot{S}_{cond} + \dot{S}_{abs} + \dot{S}_{RHX} + \dot{S}_{SHX} + \dot{S}_p + \dot{S}_{V1} + \dot{S}_{V2} \quad (23)$$

where N is the number of SAARS components. The ratio of the entropy generation rate in the selected component to  $\dot{S}_{tot}$  of the system is defined as non-dimensional entropy generation of the component and can be expressed as follows:

$$\Phi_i = \frac{S_i}{S_{tot}} \quad (24)$$

Refrigeration system is usually characterized by coefficient of performance. The COP and Carnot coefficient of performance ( $COP_c$ ) are obtained by [27,28].

$$COP = \frac{\dot{Q}_{evp}}{\dot{Q}_{gen} + \dot{W}_p} \quad (25)$$

$$COP_c = \left( \frac{T_{gen} - T_{abs}}{T_{gen}} \right) \left( \frac{T_{evp}}{T_{cond} - T_{evp}} \right) \quad (26)$$

The solar collector efficiency can be defined as

$$\eta_{sc} = \frac{Q_{sc}}{A_{sc} \cdot I} \quad (27)$$

For a solar assisted absorption refrigeration cycle, the input parameters of SAARS are the known values of  $T_{gen}$ ,  $T_{evp}$ ,  $T_{cond}$  and  $T_{abs}$  within the following temperature ranges: generator (80-100°C), evaporator (3-15°C), condenser and absorber temperatures were taken from 35 to 45°C. For the parametric investigation of the system, a computer program was developed using MATLAB. The thermodynamic properties of the LiBr-H<sub>2</sub>O solution were adopted from Patek and Klomfar [29]. The properties of water can be determined by applying an internal procedure in the simulation model using equations of Talbi and Agnew [30]. The performance of solar collector calculations is based on Abdulateef [31]. In order to simplify the simulation model, the following assumptions are adapted.

- i. All data of the system is made under steady state
- ii. The reference state of the environment condition is assumed  $T_o=25^\circ\text{C}$  and  $P_o=1$  atm.
- iii. The expansion process is assumed at constant enthalpy in the expansion device.
- iv. The incident solar radiation ( $Q_{rad}$ ) is  $700 \text{ W/m}^2$
- v. The temperature difference of  $10^\circ\text{C}$  is considered between collector and generator [28]
- vi. Condenser and absorber cooling water temperatures at inlet and exit are assumed equal to  $T_{cond}-10^\circ\text{C}$  and  $T_{cond}-5^\circ\text{C}$  and  $T_{abs}-10^\circ\text{C}$  and  $T_{abs}-5^\circ\text{C}$ , respectively
- vii. The water enters the evaporator at  $T_{evp}+15^\circ\text{C}$  and leaves at  $T_{evp}+7^\circ\text{C}$
- viii. For evacuated solar collector, we adopted the values of average heat removal factor  $F_R(\tau\alpha)=0.8$  and coefficient of heat loss  $F_RUL=2.0 \text{ W/m}^2.\text{K}$  [32]

#### 4. Results and Discussion

The results obtained from the first law analysis of the SAARS are presented in Table 1 and 2. The input parameters of simulation were taken as  $T_{gen}=90^\circ\text{C}$ ,  $T_{evp}=5^\circ\text{C}$ ,  $T_{cond}=38^\circ\text{C}$ ,  $T_{abs}=40^\circ\text{C}$ ,  $\eta_p=90\%$ , and  $\varepsilon_{SHX}=\varepsilon_{RHX}=70\%$ . The cooling capacity is 10 kW. The highest values of thermal load is observed at the generator while the load at the condenser is more than in the evaporator because of the superheating property for the inlet water vapour of the condenser. The work of the solution pump is very low as compared to other rates of the rest components. The  $COP$  values of the SAARS is 0.747 and the efficiency of the collector is up to 59% at the specified conditions. As observed in Figure 2, the ideal Carnot efficiency of the system is significantly higher than the actual performance due to the high rates of the destruction rates occurred. The  $COP$  value has a tendency to slightly increase at generator temperature about  $82^\circ\text{C}$ . The collector efficiency gets reduced when the generator temperature increases.

The entropy generation rate and the non-dimensional entropy generation of individual component are shown in Figure 3. The largest loss (75.83%) occurs in the collector followed by the generator (7%), the absorber (6.63%), the evaporator (5.45%) and the condenser (3.25%). The irreversibility of the solar collector plays the biggest part of the total irreversibility in the system regardless the operation conditions. It is clear that the highest losses rates in the generator and absorber because of the mixing process with large temperature difference. The large destruction losses of these components make their design needs more improvements. The rest of the irreversible losses are small compare to other components.

**Table 1**  
 Thermodynamics data of SAAR for Figure 1

Point	$T$ (°C)	$P$ (kpa)	$h$ (kJ/kg)	$S$ (kJ/kg.K)	$\dot{m}$ (kg/sec)	$X$ (kg/kg sol)
1	40	0.873	106.088	0.231	0.049	0.578
2	39.915	6.633	106.123	0.230	0.049	0.578
3	69.69	6.633	164.824	0.409	0.049	0.578
4	90	6.633	230.129	0.485	0.045	0.632
5	54.941	6.633	165.951	0.298	0.045	0.632
6	54.8301	0.873	165.951	0.298	0.045	0.632
7	90	6.633	2669.121	8.587	0.004	0
8	38	6.633	159.319	0.546	0.004	0
9	27.601	6.633	116.105	0.404	0.004	0
10	27.601	0.873	116.105	0.404	0.004	0
11	5	0.873	2510.452	9.025	0.004	0
12	28.1	0.873	2553.666	9.174	0.004	0
13	28	3.783	117.481	0.409	0.501	0
14	33	3.783	138.405	0.478	0.501	0
15	30	4.247	125.852	0.437	0.617	0
16	35	4.247	146.772	0.505	0.617	0
17	20	2.339	83.972	0.297	0.298	0
18	12	2.339	50.416	0.181	0.298	0
19	105	120.902	440.045	1.362	0.635	0
20	100	120.902	418.975	1.306	0.635	0

**Table 2**  
 Analysis results of the system

Components	Heat transfer rate (kW)
Solar collector ( $Q_{sc}$ )	12.36
Generator ( $Q_{gen}$ )	13.382
Evaporator ( $Q_{evp}$ )	10
Condenser ( $Q_{ond}$ )	10.482
Absorber ( $Q_{abs}$ )	12.902
Solution heat exchanger ( $Q_{SHX}$ )	2.873
Refrigerant heat exchanger ( $Q_{RHX}$ )	0.181
Pump ( $\dot{W}_p$ )	0.002
Coefficient of performance (COP)	0.747
Carnot coefficient of performance ( $COP_c$ )	1.161
Collector efficiency ( $\eta_{sc}$ )	0.59

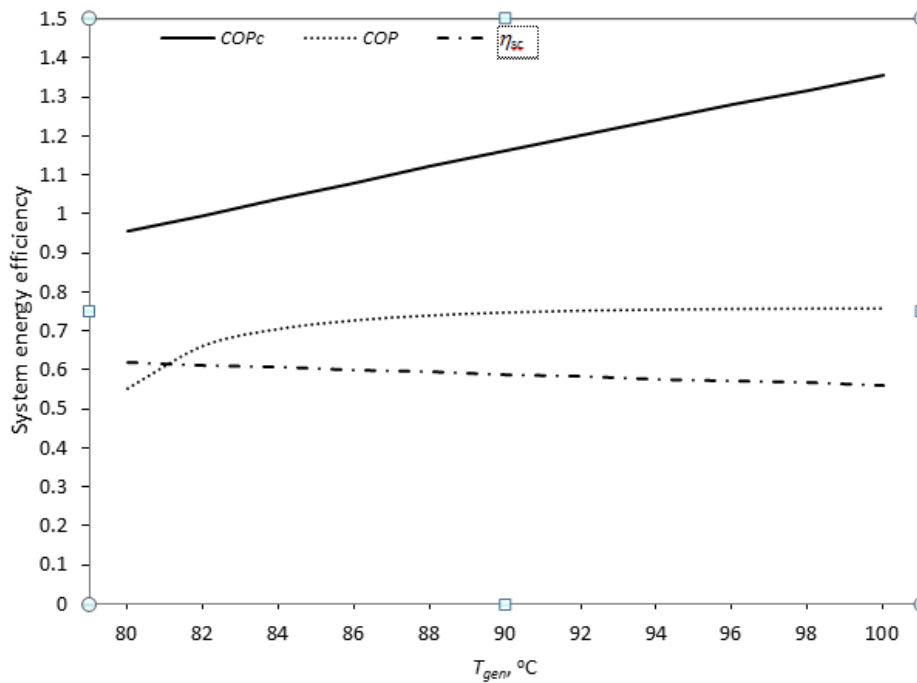


Fig. 2. Performance parameters of SAARS

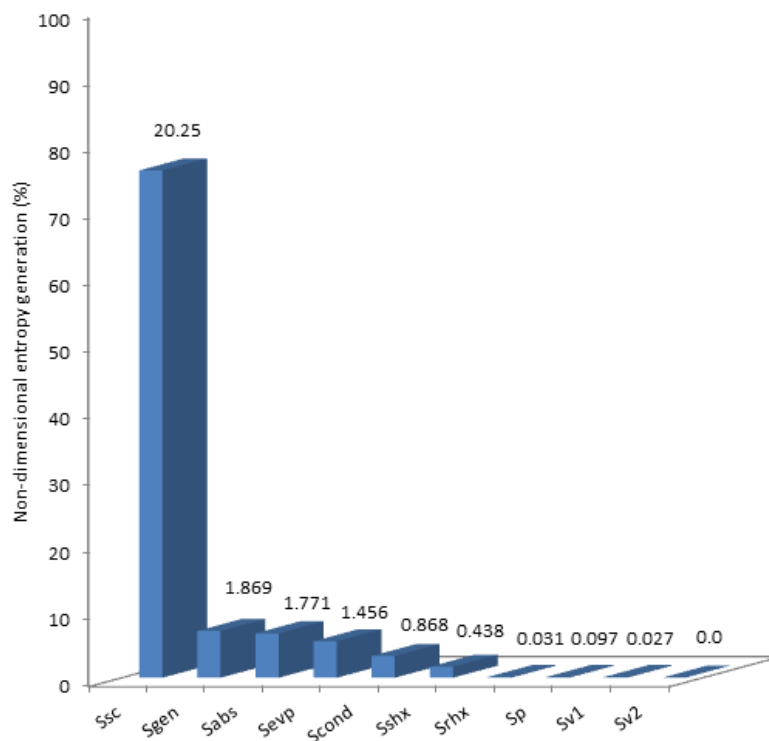
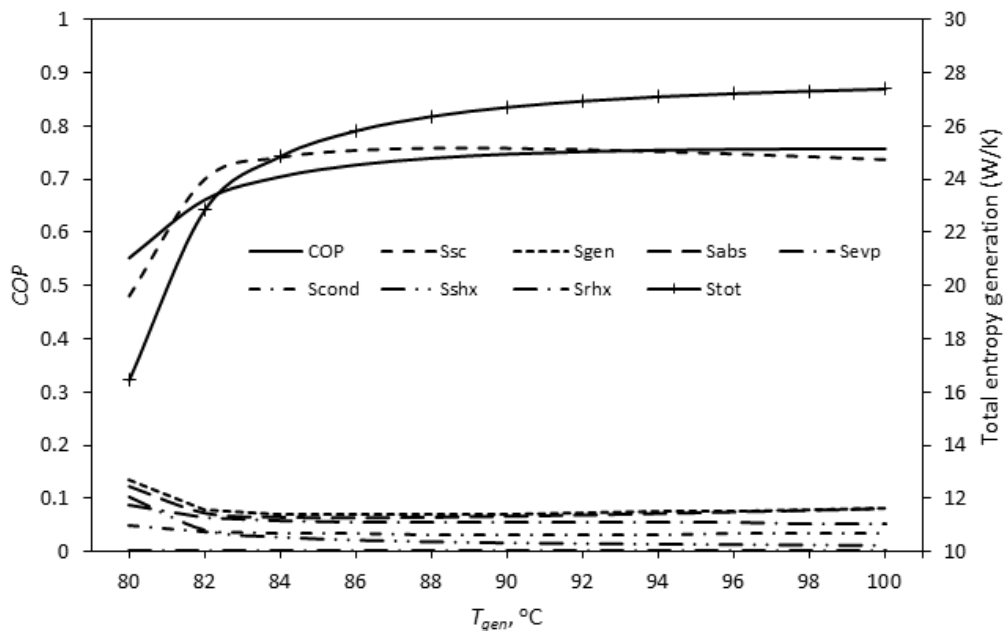


Fig. 3. Entropy generation distribution in the SAARS

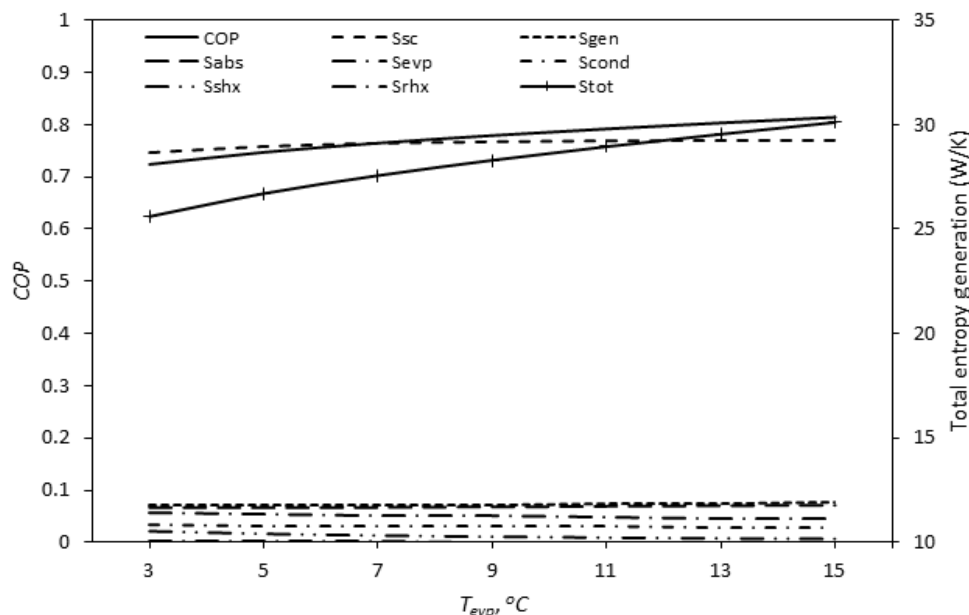
Figure 4 to 7 show the variation of the  $COP$  and the entropy generation distribution of the SAARS for a range of specified operating temperatures. Figure 4 shows the variation of the  $COP$  and the entropy generation with the generator temperature. It is clear that both  $COP$  and  $\dot{S}_{tot}$  increase with an increase in the generator temperature. This observation doesn't conform to our expectation, since a more efficient system is expected to have a higher  $COP$  and less entropy generation. This is because the most significant energy dissipation occurs in the solar collector regardless of operating conditions

as can be seen later. The values of  $\dot{S}_{tot}$  of the whole system is between 16 and 27 W/K and the largest energy dissipation found in the collector, followed by the generator and absorber. The solar collector irreversibility is between 48% and 74 % of the total entropy generation. The irreversibility of both generators and absorbers within the range of (6-14 %) of the total entropy generation. The largest irreversibility is found in these components due to the fact of high temperature difference between the solution and external fluid which causes to long finite time of heat transfer irreversibility. The increase of effectiveness of these components can reduce the temperature difference between external fluid and the solution.



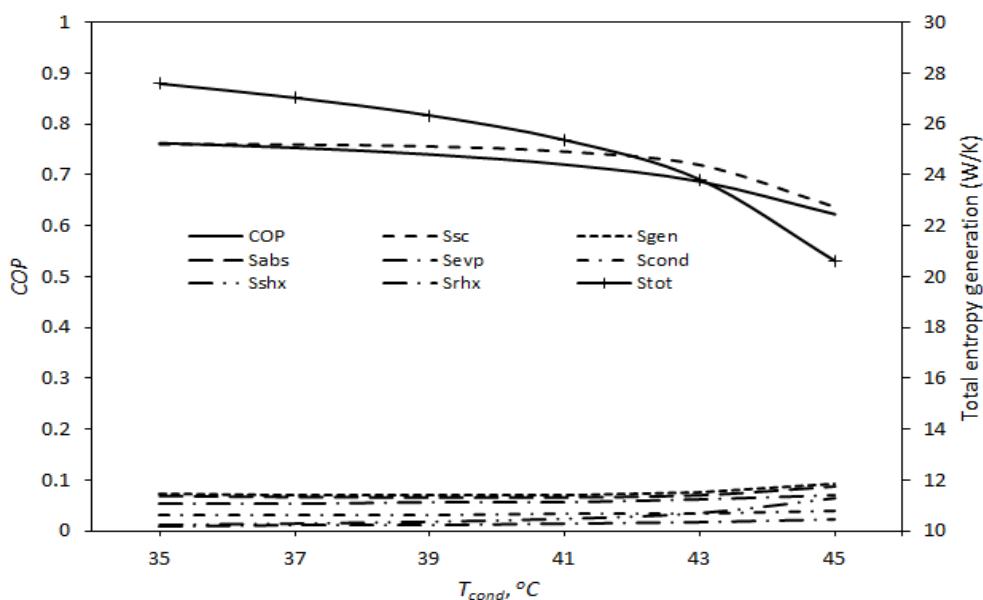
**Fig. 4.** Variation of *COP* and entropy generation with the generator temperature

Figure 5 shows the *COP* and entropy generation distribution of the system as a function of evaporator temperature. It can be observed when the evaporator temperature goes up, the *COP* and  $\dot{S}_{tot}$  of the system rises. The evaporator temperature has slightly effect on entropy generation of solar collector which makes (~75 %) of the total destruction of the system. Variation of the evaporator temperature has greater impact than the generator temperature on total irreversibility and it is about 25-30 W/K. While the irreversibility of both generator and absorber remain approximately stable, the irreversibility of the rest components slightly decreases with evaporator temperature. The rest of the irreversible losses are very low, and their impacts on the overall irreversible losses rate are inconsiderable.



**Fig. 5.** Variation of *COP* and entropy generation with the evaporator temperature

Figure 6 and 7 show the variation of *COP* and  $\dot{S}_{tot}$  of the SAARS with the condenser and absorber temperature respectively. In Figure 6, the *COP* decreases with an increase in the condenser temperature. The thermal load of the generator increases with the rise of condenser temperature which reduce the time of heat dissipation in both solar collector and generator and the *COP* gets reduced. Thus, the total irreversibility decreases gradually up to this temperature. The changes in irreversibility of condenser remain approximately stable around 3.5 % of the total irreversibility in the system. The entropy generation in the rest components slightly changes with the condenser temperature. It is clear that the variation of the condenser temperature has no great effect on entropy generation of the system components. As shown in Figure 7, the influence of absorber temperature is similar to condenser temperature. In general, the *COP* reaches high values when the system operates at high generator and evaporator temperature and low values of condenser and absorber temperature.



**Fig. 6.** Variation of *COP* and entropy generation with the condenser temperature

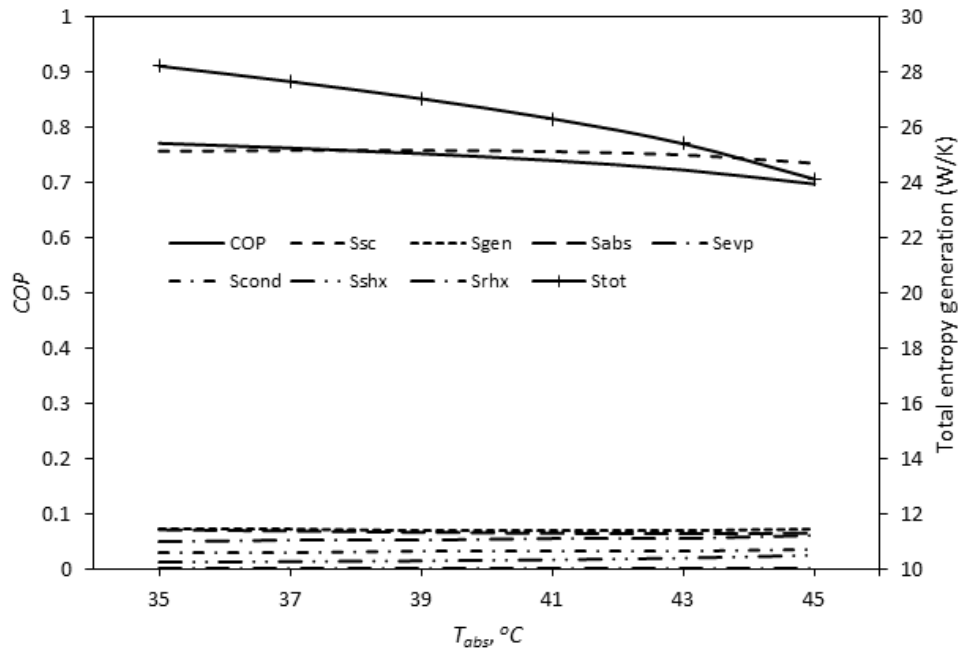


**Fig. 7.** Variation of *COP* and entropy generation with the absorber temperature

Figure 8 shows the variation of *COP* and the entropy generation distribution with the effectiveness of *SHE*. It is clear that the *COP* increases with effectiveness. The thermal load of the generator and absorber decrease with an increase in the effectiveness of *SHX* and the performance of the system gets better. Thus, the entropy generation in solar collector increases with effectiveness, and as a result of this, the  $\dot{S}_{tot}$  rate rises up. It can be noted that the system performance and entropy generation distribution is more sensitive to the effectiveness of solution heat exchanger which makes it as one of the important components in the system.

Figure 9 shows the variation of *COP* and distribution of the entropy generation of the *SAARS* with refrigerant heat exchanger effectiveness. The irreversibility of the system components unchanged with the variation of *RHX* effectiveness. Thus, the *COP* and  $\dot{S}_{tot}$  remain unchanged with effectiveness. The irreversible losses in refrigerant heat exchanger, pump and expansion valves are relatively smaller and their impacts on the total irreversibility are very low.

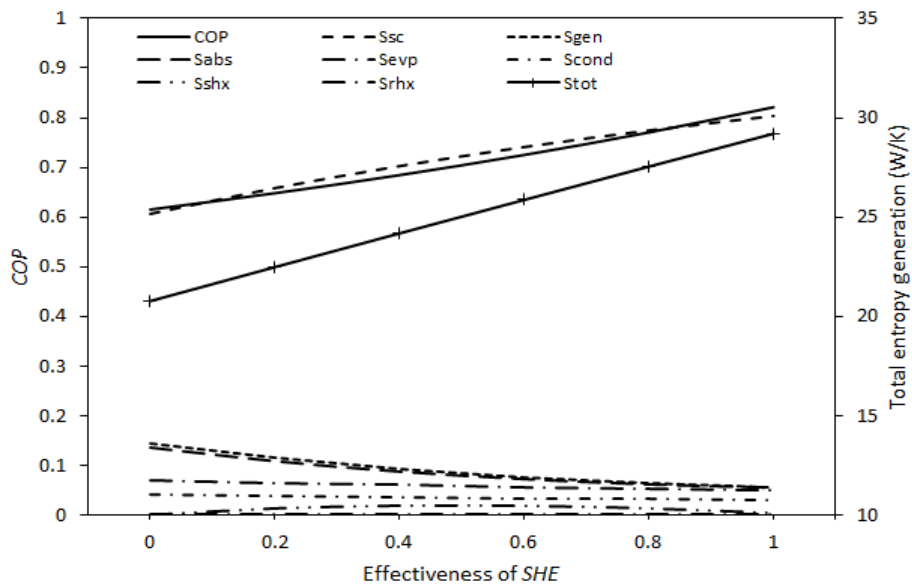


**Fig. 8.** Variation of *COP* and entropy generation with the *SHX*

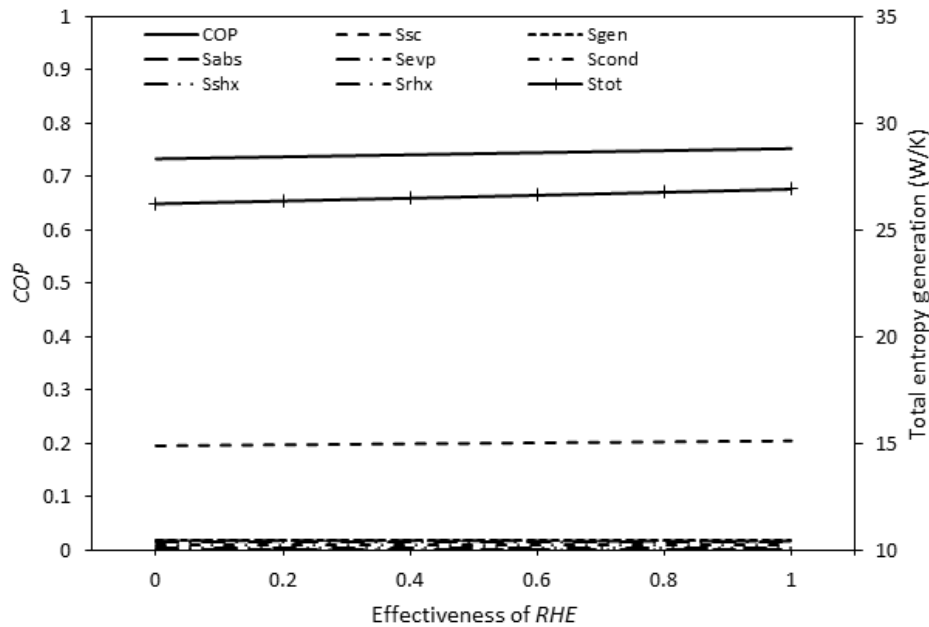


Fig. 9. Variation of COP and entropy generation with the RHX

## 5. Conclusions

The thermodynamic analysis was applied to quantify the irreversibility of each component of a SAARS. A computer simulation model was used to predict the effects of the operating temperatures and effectiveness of both SHX and RHX on the irreversible losses of each components,  $\dot{S}_{tot}$  and COP of the system. The results show that, both COP and  $\dot{S}_{tot}$  increase with the generator and evaporator temperature. The COP and  $\dot{S}_{tot}$  are inversely proportional to the condenser and absorber temperatures. The most significant thermodynamic losses dissipation takes place in the solar collector regardless of operating conditions followed by the generator, the absorber. The largest irreversibility is found in these components due to the temperature difference between the external fluid and the working fluid. Thus, a special attention should be given to these components based on their design to improve the system performance. It's also found that the COP and  $\dot{S}_{tot}$  is more sensitive to change of SHX effectiveness which makes that the SHX is one of the important components of SAARS. Moreover, energy dissipation in refrigerant heat exchanger, expansion valves and pump is very small fractions of the total energy dissipation in the SAARS. Finally, the thermodynamic analysis based on second law is a powerful tool for determining location and magnitudes of the high destruction rates.

## References

- [1] Abdulateef, J., K. Sopian, W. Kader, B. Bais, R. Sirwan, B. Bakhtyar, and O. Saadatian. "Economic analysis of a stand-alone PV system to electrify a residential home in Malaysia." In *Advances in fluid mechanics and heat & mass transfer conference*, pp. 169-174. 2012.
- [2] Hashim, Ghasaq Adheed, and NA Che Sidik. "Numerical study of harvesting solar energy from small-scale asphalt solar collector." *Journal of Advanced Research Design* 2 (2014): 10-19.
- [3] Florides, Georgios A., Savvas A. Tassou, Soteris A. Kalogirou, and L. C. Wrobel. "Review of solar and low energy cooling technologies for buildings." *Renewable and Sustainable Energy Reviews* 6, no. 6 (2002): 557-572.
- [4] Abdulateef, Jasim, Mohammed Alghoul, Azami Zaharim, and Kamaruzzaman Sopian. "Experimental investigation on solar absorption refrigeration system in Malaysia." In *Proceedings of the 3rd Wseas Int. Conf. On Renewable Energy Sources*, pp. 267-271. 2009.

- [5] Abdulateef, J. M., Nurul Muiz Murad, M. A. Alghoul, Azami Zaharim, and Kamaruzzaman Sopian. "Experimental study on combined solar-assisted ejector absorption refrigeration system." In *Proceedings of the 4th WSEAS international conference on Energy and development-environment-biomedicine*, pp. 162-166. 2011.
- [6] Sidik, NA Che, and O. Adnan Alawi. "Computational investigations on heat transfer enhancement using nanorefrigerants." *Journal of Advanced Research Design* 1, no. 1 (2014): 35-41.
- [7] Lieb, Elliott H., and Jakob Yngvason. "A fresh look at entropy and the second law of thermodynamics." In *Statistical Mechanics*, pp. 365-370. Springer, Berlin, Heidelberg, 2000.
- [8] Lior, Noam, and Na Zhang. "Energy, exergy, and second law performance criteria." *Energy* 32, no. 4 (2007): 281-296.
- [9] Ghaderian, J., C. N. Azwadi, and H. Mohammed. "Modelling of energy and exergy analysis for a double-pass solar air heater system." *Journal of Advanced Research in Fluid Mechanics and Thermal Sciences* 16, no.1 (2015): 15-32.
- [10] Chen, Jincan, and Jan A. Schouten. "Optimum performance characteristics of an irreversible absorption refrigeration system." *Energy conversion and management* 39, no. 10 (1998): 999-1007.
- [11] Sözen, Adnan. "Effect of heat exchangers on performance of absorption refrigeration systems." *Energy Conversion and Management* 42, no. 14 (2001): 1699-1716.
- [12] Chua, H. T., H. K. Toh, and K. C. Ng. "Thermodynamic modeling of an ammonia-water absorption chiller." *International Journal of Refrigeration* 25, no. 7 (2002): 896-906.
- [13] Hasan, Afif Akel, D. Yogi Goswami, and Sanjay Vijayaraghavan. "First and second law analysis of a new power and refrigeration thermodynamic cycle using a solar heat source." *Solar Energy* 73, no. 5 (2002): 385-393.
- [14] Misra, R. D., P. K. Sahoo, S. Sahoo, and A. Gupta. "Thermoeconomic optimization of a single effect water/LiBr vapour absorption refrigeration system." *International Journal of Refrigeration* 26, no. 2 (2003): 158-169.
- [15] Kaynakli, Omer, and Recep Yamankaradeniz. "Thermodynamic analysis of absorption refrigeration system based on entropy generation." *Current Science* 92, no. 4 (2007): 472-479.
- [16] Rivera, W., J. Cerezo, and H. Martínez. "Energy and exergy analysis of an experimental single-stage heat transformer operating with the water/lithium bromide mixture." *International Journal of Energy Research* 34, no. 13 (2010): 1121-1131.
- [17] Fellah, Ali, Mouna Hamed, and Ammar Ben Brahim. "On the performance of a solar driven absorption refrigerator." *Energy and Power Engineering* 6, no. 9 (2014): 278-291.
- [18] Tubreoumya, Guy Christian, Alfa Oumar Dissa, Eloi Salmwendé Tiendrebeogo, Xavier Chesneau, Aboubacar Compaoré, Kayaba Haro, Charles Didace Konseibo, Belkacem Zeghmati, and Jean Kouliadiati. "Contribution to the Modeling of A Solar Adsorption Refrigerator under the Climatic Conditions Burkina Faso." *Energy and Power Engineering* 9, no. 2 (2017): 119-135.
- [19] Modi, Bhaumik, Anurag Mudgal, and Bhavesh Patel. "Energy and exergy investigation of small capacity single effect lithium bromide absorption refrigeration system." *Energy Procedia* 109 (2017): 203-210.
- [20] Grosu, Lavinia, Andreea Marin, Alexandru Dobrovicescu, and Diogo Queiros-Conde. "Exergy analysis of a solar combined cycle: organic Rankine cycle and absorption cooling system." *International Journal of Energy and Environmental Engineering* 7, no. 4 (2016): 449-459.
- [21] Tenkeng, Maurice, Paiguy Armand Ngouateu Wouagfack, Daniel Lissouck, and René Tchinda. "Exergy Analysis of a Solar Absorption Refrigeration System in Ngaoundere." *Journal of Power and Energy Engineering* 5, no. 10 (2017): 1-18.
- [22] Mohtaram, Soheil, Wen Chen, and Ji Lin. "A Study on an Absorption Refrigeration Cycle by Exergy Analysis Approach." In *IOP Conference Series: Earth and Environmental Science* 182, no. 1 (2018): 1-5.
- [23] Adewusi, S. A., and Syed M. Zubair. "Second law based thermodynamic analysis of ammonia-water absorption systems." *Energy conversion and management* 45, no. 15-16 (2004): 2355-2369.
- [24] Ezzine, N. Ben, M. Barhoumi, Kh Mejri, S. Chemkhi, and A. Bellagi. "Solar cooling with the absorption principle: first and Second Law analysis of an ammonia-water double-generator absorption chiller." *Desalination* 168 (2004): 137-144.
- [25] Kaushik, S. C., and Akhilesh Arora. "Energy and exergy analysis of single effect and series flow double effect water-lithium bromide absorption refrigeration systems." *International journal of Refrigeration* 32, no. 6 (2009): 1247-1258.
- [26] Bejan, Adrian, George Tsatsaronis, Michael Moran, and Michael J. Moran. *Thermal design and optimization*. John Wiley & Sons, 1996.
- [27] Bejan, Adrian. *Advanced engineering thermodynamics*. John Wiley & Sons, 2016.
- [28] Pridasawas, Wimolsiri, and Per Lundqvist. "An exergy analysis of a solar-driven ejector refrigeration system." *Solar energy* 76, no. 4 (2004): 369-379.

- 
- [29] Patek, J., and J. Klomfar. "A computationally effective formulation of the thermodynamic properties of LiBr–H<sub>2</sub>O solutions from 273 to 500 K over full composition range." *International Journal of Refrigeration* 29, no. 4 (2006): 566-578.
- [30] Talbi, M. M., and B. Agnew. "Exergy analysis: an absorption refrigerator using lithium bromide and water as the working fluids." *Applied Thermal Engineering* 20, no. 7 (2000): 619-630.
- [31] Abdulateef, J. M. "Combined solar-assisted ejector absorption refrigeration system." *Department of Mechanical and Materials Engineering. Bangi, Malaysia, Univeristi Kebangsaan Malaysia Doctoral* (2010).
- [32] Flechon, J., R. Lazzarin, B. Spinner, M. Dicko, W. Charters, H. Kleinmeier, and M. A. Hammad. "Guild to solar refrigerators for remote areas and warm countries." *Paris: International Institute of Refrigeration (IIR)* (1999).